Influence of alloying on the electron momentum density in the Cu-Ni system

C. Metz and Th. Tschentscher*
European Synchrotron Radiation Facility (ESRF), Boîte Postale 220, 38043 Grenoble, France

T. Sattler, K. Höppner, and J. R. Schneider
Hamburger Synchrotronstrahlungslabor (HASYLAB) at Deutsches Elektronen-Synchrotron (DESY), Notkestrasse 85, 22603 Hamburg, Germany

K. Wittmaack
GSF-Forschungszentrum für Umwelt und Gesundheit, Institut für Strahlenschutz, 85764 Neuherberg, Germany

D. Frischke and F. Bell
Sektion Physik der Universität München, Am Coulombwall 1, 85748 Garching, Germany
(Received 27 April 1999)

We report on the measurement of the three-dimensional electron momentum density (EMD) of a 22 nm Cu/22 nm Ni sandwich foil and of a $Cu_{0.50}Ni_{0.50}$ alloy film with the same thickness, which was obtained from an identical sandwich by interdiffusion. The EMD's were measured by coincident detection of a Compton scattered photon with its recoil electron. The experiments were performed at the High-Energy beamline of the European Synchrotron Radiation Facility. The experimentally observed small change of the EMD due to alloying is reproduced by the Korringa-Kohn-Rostoker coherent-potential approximation scheme [Benedek *et al.*, Phys. Rev. B **32**, 7650 (1985)]. [S0163-1829(99)08143-6]

I. INTRODUCTION

For quite a long time Compton scattering has been used to characterize the electron momentum density (EMD) of valence electrons in solids.[1] The double-differential cross section describing the energy and angular distribution of inelastically scattered hard x-rays is proportional to the so-called Compton profile (CP), which is defined as a twofold integration over the EMD. This integration results from the lack of information about the momentum distribution of the recoiling electrons. Since integration averages over large volumes in momentum space, detailed information about solid-state effects like the influence of alloying in compound systems might become difficult to obtain. It is therefore desirable to measure the EMD directly by fixing the scattering kinematics: if the momentum of the recoiling electron is measured simultaneously with that of the scattered x-ray photon, the momentum of the electron in its initial state can be reconstructed in a unique way. The corresponding triple-differential cross section is proportional to the EMD itself.[2–5] The main difficulty of such a $(\gamma,e\gamma)$ coincidence experiment originates from the strong incoherent elastic scattering of the recoiling electron within the target, which disturbs the determination of the recoil momentum by multiple scattering. Since the mean free path for elastic scattering of electrons with an energy of 50 keV in Cu is only about 12 nm,[6] targets as thin as possible are required.

In this paper we will report on the influence of alloying by comparing the EMD of $Cu_{0.50}Ni_{0.50}$ with those of its pure constituents. The electronic structure of this transition-metal solid-solution alloy has received extensive attention. The Cu-Ni system is completely soluble over the whole concentration range, i.e., there is no miscibility gap yielding single phase disordered fcc alloys. The lattice parameter changes between Cu and Ni by 2% only and the density by 0.3%.[7] Thus, a change of the electronic structure will not be obscured by geometrical effects. Substantial improvement has been achieved in the theoretical understanding of the electronic structure of disordered alloys using a general multiple-scattering formalism. Three principal approximations have been investigated: (i) the virtual-crystal approximation (VCA), where the effective potential of the alloy is the average of that of the pure constituents; (ii) an average *t*-matrix approximation; and (iii) the coherent-potential approximation (CPA), where a self-consistency requirement is introduced to obtain the single-site *t* matrix.[8,9] It is this property of the CPA that makes it preferable to apply, especially for alloys of high concentrations. The underlying Green's-function technique of the multiple-scattering problem is similar to that of the Korringa-Kohn-Rostoker (KKR) theory.[10,11] In a series of papers Bansil and co-workers[12–17] have extensively investigated the Cu-Ni system theoretically. In addition, Temmerman, Gyorffy, and Stocks[18] have used KKR-CPA for a detailed study of the Bloch spectral function in these alloys. On the experimental side poly-crystalline Cu_xNi_{1-x} alloys have been investigated by conventional Compton scattering,[19] and the CP's were compared with those from KKR-CPA calculations. Qualitative agreement was found, though at small momenta the influence of alloying was predicted by theory to be stronger than revealed by experiment. Differences of Cu_xNi_{1-x} directional Compton profiles provided by investigations of single crystals[20] have been compared with relativistic KKR-CPA calculations. Whereas the calculations cited above hold for paramagnetic alloys only, this new computation includes the ferromagnetic behavior of Ni-rich alloys. Especially at momenta below 0.5

a.u., the experimental anisotropies are not well described by theory.

A method that also measures EMD's is angular correlation of annihilation radiation (ACAR), though, strictly speaking, it measures the electron-positron pair density, i.e., the electron momentum space wave function weighted by the positron wave function within the solid.[21] Until now only long-slit experiments, i.e., 1D-ACAR (Ref. 22) or investigations with the crossed-slit geometry,[23–26] have been reported for the Cu-Ni system, but no complete 2D-ACAR experiment. The main topic of these early investigations was the reduction of the Fermi surface (FS) extension with increasing Ni concentrations, especially the decrease of the neck radius at the L point of the Brillouin zone. The change of the FS by alloying in the Cu-Ni system is fairly well described by KKR-CPA theory.[27,28]

II. METHOD

If a photon with energy ω and momentum $\mathbf{k}$ is scattered at an electron with band energy $\varepsilon>0$ and momentum $\mathbf{p}$, the final photon energy ω' and momentum $\mathbf{k}'$ is connected with the final electron energy E' and momentum $\mathbf{p}'$ via energy and momentum conservation

$$\varepsilon(\mathbf{p})=\omega-\omega'-E', \tag{2.1a}$$

$$\mathbf{p}=\mathbf{k}'+\mathbf{p}'-\mathbf{k}. \tag{2.1b}$$

Thus, if $\mathbf{k}$, $\mathbf{k}'$, and $\mathbf{p}'$ are known experimentally, the initial momentum $\mathbf{p}$ can be reconstructed in a unique way. This demands the coincident detection of both the scattered photon $(\omega',\mathbf{k}')$ and the recoil electron $(E',\mathbf{p}')$. The coincidence count rate will be proportional to the triple-differential cross section, which can be written within the so-called impulse approximation:

$$\frac{d^3\sigma}{d\omega' d\Omega_\gamma d\Omega_e}=\frac{\omega}{\omega'}p'\left(\frac{d\sigma}{d\Omega}\right)_{\mathrm{KN}}\rho(\mathbf{p}), \tag{2.2}$$

where $(d\sigma/d\Omega)_{\mathrm{KN}}$ is the Klein-Nishina cross section for linearly polarized photons and $\rho(\mathbf{p})$ is the EMD. Since our experiment cannot distinguish between different valence bands, $\rho(\mathbf{p})$ is the total EMD, i.e., summed over all electronic states. The basic idea of the experiment is the following: first, a double layer (sandwich) consisting of equal amounts of pure Cu and Ni is investigated, yielding the average EMD $\rho=(\rho_{\mathrm{Cu}}+\rho_{\mathrm{Ni}})/2$. The sample then is heated such that complete interdiffusion takes place. Since the Cu-Ni system has no miscibility gap, a homogeneous alloy is formed that again is measured in order to obtain the EMD of the alloy. The influence of alloying is studied by taking the difference of both experiments. Due to the multiple-scattering problem, very thin foils have to be used, and therefore interdiffusion occurs within moderate times at not too high temperatures.

III. EXPERIMENT

The experiment was performed at the High-Energy X-Ray Scattering beamline ID15A of the European Synchrotron Radiation Facility ESRF.[29] An asymmetric wiggler with seven periods and strong poles of 1.8 T was used with a critical energy of 44.1 keV. The white beam was monochromatized by a (220) bent Si crystal in Laue geometry. The photon energy was $\omega=146$ keV with $\Delta\omega=0.71$ keV full width at half maximum (FWHM). The photon beam entered an evacuated target chamber (10^{-3} Pa) with an externally mounted intrinsic Ge-diode (energy resolution 0.4 keV FWHM at 100 keV) at a scattering angle $\theta=140°$. Thus, the scattered photon energy was about 97 keV and the electron recoil energy 49 keV. The electrons were measured by a two-dimensional position sensitive detector, which consisted of 16×16 individual photodiodes (Fig. 1). The center of the array was placed in the direction of the momentum-transfer vector $\mathbf{q}_0=\mathbf{k}-\mathbf{k}_0'$, where $\mathbf{k}_0'$ is the momentum of photons scattered at electrons at rest. Since both the energy resolution of the photon and electron detector are large compared to the binding energy ε of the valence electrons, which dominate the EMD, the latter has been neglected in Eq. (2.1a). Detailed Monte Carlo (MC) simulations of the momentum resolution included the correlated scattering due to the cross section of Eq. (2.2), solid angle and energy resolution of the Ge diode, energy broadening of the primary beam, and extension of the beam spot at the target. The variance vector for the momentum uncertainties in the three Cartesian directions of momentum space obtained by these MC calculations was $\sigma_{\mathbf{p}}=0.14,0.38,0.19$ a.u. Here p_z is parallel to $\mathbf{q}_0$, p_x lies in the $(\mathbf{k},\mathbf{k}')$ scattering plane, and p_y is perpendicular to it. Emission patterns of the recoiling electrons were recorded by the 2D electron detector with a granularity of about 0.14 a.u. in p_x and 0.28 a.u. in p_y direction. Thus, the variance in p_x and p_y direction extended over approximately 1 pixel. The time resolution of the coincidence circuit was about 200 ns, considerably larger than the bunch distance of 3 ns in the so-called 2/3 fill mode of the ESRF. Time correlation spectra showed very little chance coincidences, which nevertheless were taken into account. The overall coincidence rate due to a primary beam of about 2×10^{11} photons/s was about 2 Hz. A total of 1.4×10^6 coincidence events for each experiment was accumulated.

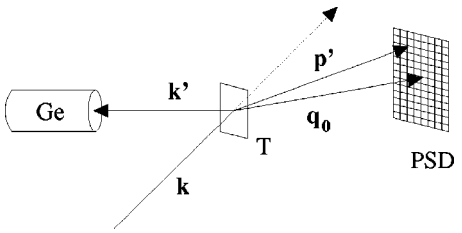

FIG. 1. Experimental setup: Ge, Ge diode; T, target; PSD, position sensitive electron detector.

Since self-supporting Cu or Ni foils with diameters of 8 mm and thicknesses of 20 nm cannot be prepared, we have evaporated 22 nm Cu followed by 22 nm Ni on a 30 nm thin C-foil acting as a backing. The backing was made by condensation of evaporated carbon atoms on a thin betaine film that had a fine crystalline-like structure that acted as a replica for the carbon backing and guaranteed a high mechanical stability. Finally, the betaine substrate was dissolved in water, and the carbon film was mounted on a frame. Both Cu and Ni were evaporated on the free-standing carbon backing with a rate of about 0.5 nm/s, and the films condensated at

room temperature. In order not to lose beam time by the heating procedure, we decided to prepare two sandwich foils simultaneously where the second was heated at about 500°C for 2 h and then furnace cooled. The data of Almazouzi *et al.*[30] yield a diffusion coefficient of about $D=2\times10^{-19}$ m^2/s giving for a heating time of $t=7\times10^3$ s a diffusion length $x=2\sqrt{Dt}=80$ nm. This is four times the Cu (or Ni) thickness. Since the diffusion coefficient holds for single crystals, we believe that this diffusion length is a lower limit only. It is well known that especially at rather low temperatures (500°C) pipe diffusion along grain boundaries or dislocations can be orders of magnitude faster than volume diffusion.[31] Experimental details of this type of diffusion in the Cu-Ni system can be found in Refs. 32–34. Since we expect that our sandwich foils contain quite a lot of defects like grain boundaries and dislocations, diffusion short circuits starting from these defects within the foils will occur and thus shorten the effective diffusion time for complete interdiffusion substantially. The data of Almazouzi *et al.*[30] refer to the diffusion of Ni into a Cu single crystal. Although the diffusion coefficient of Cu into a Ni matrix is about three orders of magnitude smaller than that of Ni into Cu at 500 °C (Ref. 35), we expect no void formation due to the Kirkendall effect[36] at the backing-alloy interface. This is supported by our experience that also after heating the alloy film did not lose its good mechanical contact with the carbon substrate. But it cannot be excluded that vacancy precipitation takes place inside the alloy. The diffusion coefficients cited above are so-called impurity diffusion coefficients in contrast to chemical diffusion coefficients, which hold for the interdiffusion in inhomogeneous binary alloys.[36] Brunel, Cizeron and Lacombe[37] measured the chemical diffusion constant over the whole concentration range of the Cu-Ni system for temperatures between 700 °C and 1070 °C. Extrapolating their data to 500 °C yields diffusion coefficients in the range of 10^{-19} m^2/s changing by a factor of 5 over the concentration range. These findings agree with ^{63}Ni tracer diffusion in a $Cu_{0.79}Ni_{0.21}$ alloy investigated by Butrymowicz, Manning and Read[38] yielding a diffusion coefficient of the same order of magnitude.

Both foils, the sandwich and the alloy, have been characterized by x-ray fluorescence analysis (XRF), elastic recoil detection analysis (ERDA), and secondary ion mass spectroscopy (SIMS). In XRF the ratio $R=N_{Cu}/N_{Ni}$ could be determined where N_{Cu} and N_{Ni} are the atomic number densities of both elements. The $K\alpha$ lines of Cu and Ni, excited by the 146 keV primary photon beam, are well resolved by the Ge diode (except that the $K\alpha$ line of Cu is slightly contaminated by the Ni $K\beta$ line, an effect which is easily accounted for). Correcting the line intensities for the ratio of the photoelectric cross sections and the fluorescence yields the ratio R was close to unity within 2% for both foils, indicating that in fact equal amounts of Cu and Ni had been deposited on the backing. Since the foils are extremely thin, the probability that Cu $K\beta$ radiation can excite Ni K fluorescence is negligible. ERDA reveals the contamination of the targets with low-Z material. In short, 150 MeV Au ions from the Munich heavy-ion accelerator have been directed on the target foils, and the recoil ions ejected from the target have been analyzed by an ionization chamber.[39] Analysis of the nuclear charge Z of the recoil ions was achieved via the specific energy loss ΔE of the ions within the ionization chamber ($\Delta E\sim Z^2$). Since the cross section for ejectile emission is the well-known Rutherford cross section, the analysis of low-Z contaminants can be made quantitatively. Figure 2 shows a spectrum of ejectile ions from our foils. In addition to strong peaks from the C backing and the nonresolved Cu and Ni ions, the essential contaminants are oxygen and nitrogen. Quantitative analysis yields concentrations of about 5 at. % nitrogen and 7 at. % oxygen, which are slightly reduced upon heating, presumably due to desorption. Again, the relative difference of elemental composition of both foils—which is important for the later investigation of the alloy influence, where the difference of the EMD's from both targets is taken—was in the 1% region.

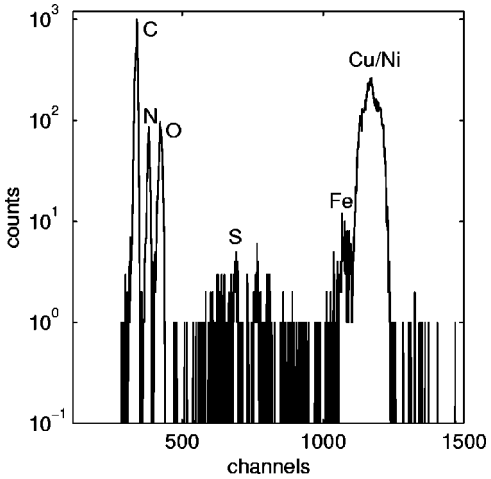

FIG. 2. Elemental composition of the sandwich target from ERDA. Elements are indicated. Cu and Ni are not resolved.

SIMS analysis aimed at determining the sample composition as a function of distance from either the Ni or the C surface side of the foils. The depth profiling measurements[40] on the free-standing foils were performed in a quadrupole based ion microprobe using a normally incident, raster scanned 2 keV O_2^+ primary ion beam for sputter erosion and secondary ion yield enhancement[41] (scan width 140 μm, electronically gated area typically 40 μm). Raster scanning ion imaging[42] in parallel with data acquisition during depth profiling provided qualitative information about the lateral uniformity in composition. Moreover, lateral differences in thickness could be assessed from the local differences in time required for complete removal of the sample (''breakthrough'').

Figure 3(a) shows examples of depth profiles of Ni (dashed line) and Cu (solid line) measured from the Ni side of the sandwich. For ease of comparison, the profiles are presented in normalized form, ignoring surface effects. As the erosion rate could not be determined independently, the profiles are shown as a function of sputtering time. The Ni and Cu layers of the sandwich are clearly separated, but the interface is not sharp. This is attributed to the lateral nonuniformity of the carbon backing, presumably related to the roughness of the betaine spacer. The nonuniformity also gave rise to differences in breakthrough time by about 10%. Within this margin, profiles measured at different spots on the sample were found to be reproducible. The effect of annealing on the sample composition is illustrated in Fig. 3(b).

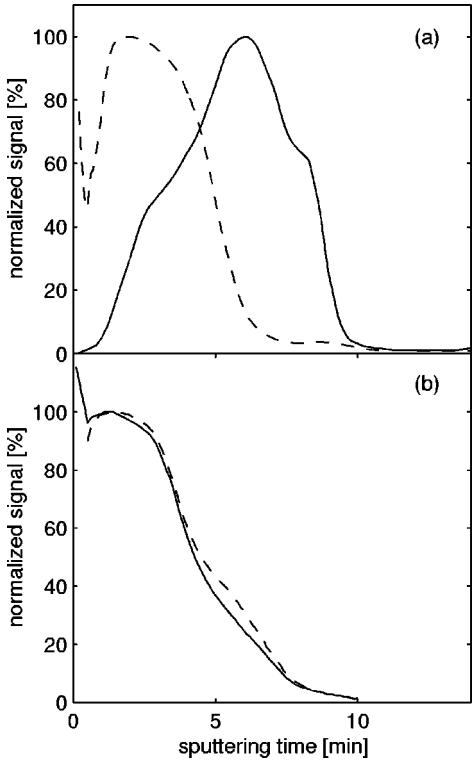

FIG. 3. Cu (solid line) and Ni (dashed line) concentration as a function of depth. (a) sandwich foil, (b) heated sandwich foil.

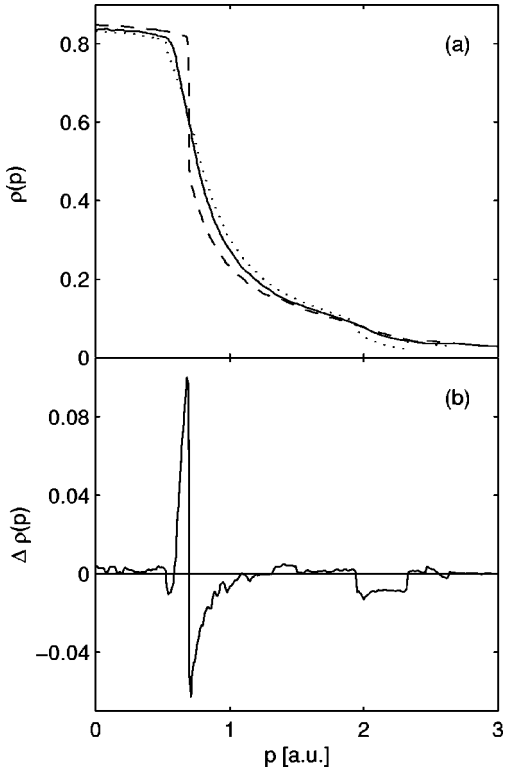

FIG. 4. The calculated EMD $\rho(p)$ of Cu (broken line), Ni (dotted line), and $Cu_{0.50}Ni_{0.50}$ (solid line) (a) and the difference $\Delta\rho$ as defined in Eq. (4.1) (b). From Ref. 19.

It is evident that, within experimental accuracy, the depth profiles of Ni (dashed line) and Cu (solid line) are identical. This result supports the idea that the heat treatment of the sandwich resulted in the formation of a uniform alloy. The same observation has been made by Röll and Reill[43] for the interdiffusion of Cu-Ni multilayers (the thickness of each layer was 45 nm) after annealing at 450 °C for 30 min and by Suni, Nicolet, and Mäenpää[44] for 150-nm-thick Cu-Ni couples heated at 550 °C for 15 min. Identical distributions of Ni and Cu were also observed in depth profiling from the carbon side of the sample. The SIMS measurements revealed some contamination with Fe, in accordance with Fig. 2. Furthermore, carbon was found to be present in the alloy at concentrations of about 3%.

Some attention has been devoted to the problem of short-ranged clustering in Cu_xNi_{1-x} alloys. Warren-Cowley short-range-order parameters have been measured by diffuse neutron scattering.[45,46] The measurements indicated that there is a fairly small tendency for Cu and Ni atoms in an alloy to prefer nearest neighbors of the same atomic species, but beyond the nearest-neighbor shell, the atomic arrangement is essentially random. Specifically, for $x=0.5$ the probability that the nearest neighbor of an atom is of the same species is 0.56 instead of 0.50. This number holds for 550 °C.[45] At first glance short-range clustering seems to contradict the absence of a miscibility gap since it is widely accepted that clustering will always precede or accompany spinodal decomposition. In fact, several authors have predicted a miscibility gap with a critical temperature below 450 °C,[46–48] but since chemical diffusion constants are extremely low at these temperatures, atomic motion is essentially frozen out and prohibits thermodynamic equilibrium. We therefore conclude from the neutron-scattering experiments that the effect of clustering is small and can be neglected.

IV. EXPERIMENTAL RESULTS AND DISCUSSION

Figure 4(a) shows the spherically averaged theoretical EMD's of $Cu_{0.50}Ni_{0.50}$ and the pure elements.[19] Whereas the constituents have rather sharp discontinuities at the Fermi breaks—the radii of 0.76 a.u. for Cu and 0.60 a.u. for paramagnetic Ni correspond roughly to the bellies of the rather spherical FS of the sixth band for both cases[49,50]—the break of the alloy is rounded off. It is well known that the eigenvalues $\varepsilon(\mathbf{p})$ of the band structure are real in a perfect crystal, but they become complex numbers in the alloy due to disorder-induced smearing of states.[9] This is in contrast of the behavior of *ordered* alloys, which can be treated by more conventional band-structure calculations.[51] The smearing implies that the alloy FS is not sharply defined but possesses a total width $2\Delta p(\varepsilon_F)$, which amounts in the 50-50 alloy to 0.04 a.u.[52] It is also seen from Fig. 4(a) that the EMD's for Ni and the alloy are remarkably more intense than that for Cu for momenta above the FS, indicating the stronger influence of the more diffuse *d* electrons in Ni and the alloy. Or, in other words, going from Ni to Cu, the Fermi surface expands and becomes more pronounced, reflecting the increase of the *s*-*p* character of the associated states. In Fig. 4(b) we have plotted the difference

$$\Delta\rho=(\rho_{\mathrm{Cu}}+\rho_{\mathrm{Ni}})/2-\rho_{\mathrm{Cu}_{0.5}\mathrm{Ni}_{0.5}}. \tag{4.1}$$

$\Delta\rho$ should be identical with the experimental accessible difference $\rho(\text{sandwich})-\rho(\text{heated sandwich})$ and shows the

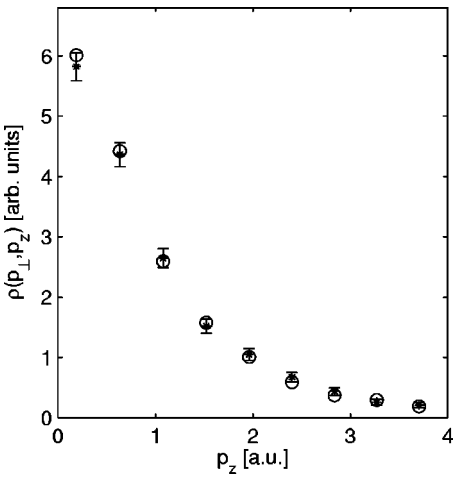

FIG. 5. The experimental EMD for the sandwich (stars) and the alloy (open circles) at $p_\perp = 0.5$ as a function of p_z.

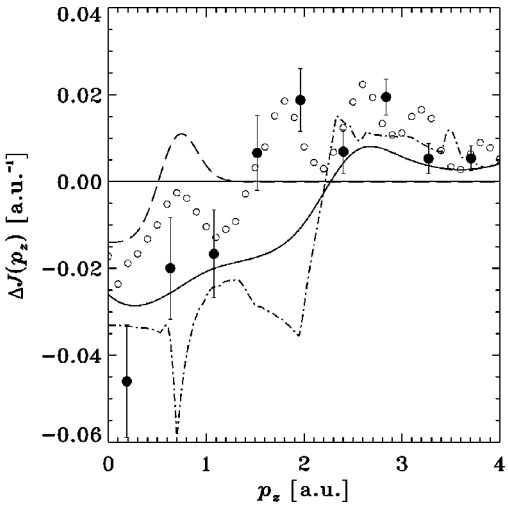

FIG. 6. The coincident CP difference ΔJ (filled circles), the noncoincident difference (open circles), and $c(p_z)/4$ from the KKR-CPA calculation (solid line) (Ref. 19). For comparison the rigid-band model (broken line) and the integration of the solid curve in Fig. 7 (dash-dotted line, not convoluted with experimental resolution) are also shown.

influence of alloying on the EMD. It is evident that the strongest effect is near the Fermi breaks, i.e., for momenta between 0.5 and 1 a.u.

In Fig. 5 both the EMD's of the sandwich (stars) and the alloy, i.e., the heated sandwich (open circles) at $p_\perp = \sqrt{p_x^2+p_y^2} = 0.5$ a.u., are plotted as a function of p_z. For this case differences should be observable near $p_z = 0$, i.e., at large count rates. The experimental points of Fig. 5 have been normalized to the total number of coincidence events in each measurement, which are orders of magnitude larger than those which yield Fig. 5. It is readily seen that no difference within the error bars can be observed. Although our targets are isotropic, it is unfortunately not possible to increase statistics by adding up the coincidence events for a constant momentum p since both the experimental resolutions in the three Cartesian directions of **p** are different (see Sec. III), and electron multiple-scattering influences the p_x, p_y components stronger than p_z. But, nevertheless, to improve statistics, we have summed up all events for a constant p_z to obtain what is called a coincident Compton profile J_{coinc}. Due to the limited range of our experiment in p_x ($\leqslant 1.6$ a.u.) and p_y ($\leqslant 2.5$ a.u.), J_{coinc} is not identical with the noncoincident CP. But in addition to the increase of the number of events, it has two other important advantages: Due to the limited (p_x, p_y) range, the contribution of core states is strongly reduced and the trigger condition provides photon spectra free of any background radiation. J_{coinc} has been evaluated in absolute units by normalizing it to the effective number Z_{eff} of electrons that contribute to it. This number has been obtained by a Monte Carlo procedure that simulates the whole experiment including electron multiple scattering and the detailed geometry of both the photon and electron detector. The EMD's of Fig. 4(a) and that of graphite[53] have been used as input data. Due to the finite extension and the granularity of the electron detector, only a fraction f_i of all recoil electrons, generated by photons scattered at the element $i = \mathrm{C}$, Cu, or Ni and detected by the γ detector, are measured. Having obtained f_i from the MC calculation we have set

$$Z_{\mathrm{eff}} = \sum_i f_i c_i Z_i , \tag{4.2}$$

where Z_i are the nuclear charges and c_i are the relative atomic concentrations of the main elements that constitute the target foil. While electron multiple scattering has some influence on Z_{eff}, a change of the shape of J_{coinc} due to this effect is negligible. This is also true if in the MC simulation the individual thicknesses of C, Cu, and Ni are increased by 50% (we know the absolute value of the thicknesses within 10% only). But in addition, only the difference of the coincident Compton profiles of the sandwich and the alloy will be discussed in the following, and therefore influences of multiple scattering should cancel, at least to first order.

Figure 6 shows the difference $\Delta J = J_{\mathrm{coinc}}(\mathrm{sandwich}) - J_{\mathrm{coinc}}(\mathrm{alloy})$ as a function of p_z (filled circles). Due to improved statistics, now an alloying effect is clearly observable. At $p_z = 0$ it amounts to about 2% of the total coincident profile, i.e., it is a rather small effect. These findings are supported by x-ray photoemission[57] and x-ray absorption spectroscopy,[54] which show that the density of states of Cu-Ni alloys can, to a very good approximation, be made up by superimposing those of Ni and Cu. This means that there is indeed only a very limited sharing of electrons by the two constituents. Though the (p_x, p_y) range is limited, it extends over the major part of the valence EMD. We therefore compare in Fig. 6 also with the experimental noncoincident CP difference[19] $\Delta J = (J_{\mathrm{Cu}} + J_{\mathrm{Ni}})/2 - J_{\mathrm{Cu_{0.5}Ni_{0.5}}}$. Despite the oscillations, the general trend of the experimental points (open circles) agrees nicely with our results. The oscillatory behavior might be an artifact introduced by the numerical procedure of data processing.[19] Neither data processing like a deconvolution procedure accompanied by frequency filtering nor background subtraction has been applied to our data. This might be viewed in light of a remark made by Bansil *et al.*[20] that in their noncoincident Compton scattering experiments on Cu-Ni single crystals absolute values of experimental CP's are difficult to interpret due to the presence of a background contribution of uncertain origin. The data of

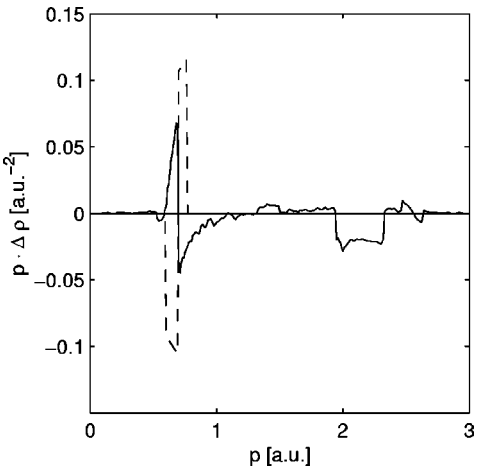

FIG. 7. $p\Delta\rho$ for the rigid-band model (broken line; multiplied by 0.5) and the KKR-CPA (solid line) as a function of momentum p.

Benedek *et al.*[19] for five Cu_xNi_{1-x} alloys and the two pure elements have been fitted by these authors to a common CP,

$$J_{\text{fit}} = a(p_z) + b(p_z)(x-0.5) + c(p_z)(x-0.5)^2. \quad (4.3)$$

With our notation one obtains $\Delta J = c(p_z)/4$. In the work of Benedek *et al.*[19] also KKR-CPA theory has been parametrized in the form of Eq. (4.3). The solid line in Fig. 6 represents $c_{\text{theory}}/4$. In view of the smallness of the effect, a very reasonable agreement between theory and experiment is observed.

For a more qualitative understanding of the alloy effect, we have also used a very simple rigid-band (RB) model,[55] which has been discussed both in photoemission[56–58] and Compton profile studies.[19] Assuming that the Fermi momentum is given by $p_F = \alpha Z^{1/3}$ where $\alpha = (3\pi^2/\Omega)^{1/3}$ (Ω: atomic volume) remains essentially the same for the elements and the alloy, the only changing parameter is the valence Z. For the RB model one has

$$Z_{\text{alloy}} = xZ_{\text{Cu}} + (1-x)Z_{\text{Ni}}, \quad (4.4)$$

which implies

$$p_F^3(\text{alloy}) = xp_F^3(\text{Cu}) + (1-x)p_F^3(\text{Ni}). \quad (4.5)$$

Inserting the experimental belly radii of the pure constituents, one arrives for $x = 0.5$ at $p_F(\text{alloy}) = 0.69$ a.u., a value which is identical with that found experimentally by the measurement of ferromagnetic exchange coupling across Cu_xNi_{1-x} layers.[59,60] (Classical techniques like the de Haas–van Alphen effect or magnetoacoustic resonance are not applicable in concentrated alloys due to electron scattering introduced by alloy disorder.[61]) Starting with the EMD for free electrons $\rho(p) = \Omega/(4\pi^3)\,\theta(p_F - p)$, where $\theta(p)$ is the step function, we have calculated the Compton profile difference ΔJ and convoluted it with our p_z resolution. The broken curve of Fig. 6 shows that this simple model is—at least for small momenta—in qualitative agreement with the experimental data. But it seems that this agreement is fortuitous. In Fig. 7 we have plotted the function $p\Delta\rho$ for both the RB model (broken curve; for better comparison we have multiplied by 0.5) and the EMD difference from KKR-CPA. It is evident that the intensity spikes at about 0.7 a.u. have a different sequence for both calculations. Integration of this function from a lower limit p_z yields the Compton profile difference

$$\Delta J(p_z) = 2\pi \int_{|p_z|}^{\infty} p\Delta\rho\, dp. \quad (4.6)$$

Whereas the Compton profile difference of the rigid-band model is determined by the EMD difference around 0.7 a.u., in KKR-CPA the corresponding contribution is small since the spikes at these momenta nearly cancel each other. In contrast, the KKR-CPA Compton profile difference $c(p_z)/4$ in Fig. 6 is dominated by the negative feature around 2 a.u. (Fig. 7). This is demonstrated by the Compton profile difference ΔJ obtained from the solid curve of Fig. 7 (dash-dotted curve in Fig. 6). It first reveals a reasonable agreement of the KKR-CPA Compton profile difference with the fitted curve $c(p_z)/4$. Second, it demonstrates the compensation of the spikes by its strong extremum at about 0.7 a.u. If the lower integration limit p_z has passed the first spike, the second one is no longer compensated yielding the strong minimum. Passing the second spike also, ΔJ is nearly at the same value as before showing that the whole effect is dominated by the feature at about 2 a.u. in Fig. 7. It results from the behavior of the Fermi breaks near the (1,1,2) reciprocal-lattice vector, which apparently survives the spherical averaging. Benedek *et al.*[19] employed the special direction method[62] and especially discussed its influence on the EMD near the Fermi breaks. In Ni rather strong X-centered hole ellipsoids in the fourth Brillouin zone dominate the Fermi surface, yielding a strong reduction of the EMD. On the contrary, for the 50-50 alloy and Cu, the Fermi energy lies above the d bands at this point, resulting in a less pronounced break.[52,15] Altogether, this leads to a negative contribution of $\Delta\rho$ at about 2 a.u. Since this feature dominates ΔJ, it may happen that due to the limited range of our detector in p_x direction our experimental points of Fig. 6 reflect a too small alloy effect. Nevertheless, we find it very remarkable that Umklapp contributions as discussed above are accessible to experimental observation.

V. SUMMARY AND PERSPECTIVES

We have measured the influence of alloying in a $Cu_{0.50}Ni_{0.50}$ alloy that has been produced by interdiffusion of 22-nm thin Cu and Ni films. Both the sandwich and the alloy have been characterized by XRF, ERDA, and SIMS. Coincident Compton profiles reveal a small difference between a simple mixing of the EMD's of the elements and that of the alloy. The effect can be explained by KKR-CPA calculations. Especially the use of ultrathin target foils opens the possibility to study a large class of random binary alloys that are produced far from thermodynamic equilibrium. Instead of producing the alloy by interdiffusion, they could be made either by simultaneous evaporation and condensation[54] of the constituents or by cosputtering. In this way arbitrary alloy compositions are achieved that would otherwise be impossible to get from the melt. On the other hand, KKR-CPA

calculations are independent from thermodynamic conditions. Cosputtered Cu_xNi_{1-x} films with x between 0.12 and 0.87 have been studied by photoemission spectroscopy[63] and found in better agreement with CPA calculations than earlier measurements[56] due to improved resolution. This demonstrates that the production method yields reasonable results. At the same time it opens the possibility to study alloys where the size of the alloying effect is larger than in Cu/Ni system, which was chosen due its complete miscibility.

ACKNOWLEDGMENTS

The authors thank Dr. W. Assmann from the Munich Heavy Ion Accelerator Group for the ERDA measurements. C.M. acknowledges a grant from the ESRF. This work was supported by the Bundesministerium für Bildung, Wissenschaft, Forschung und Technologie, Contracts Nos. 05 5WMAAI and 05 650HRA5.

*Present address: HASYLAB (DESY), Hamburg, Germany.

[1] M.J. Cooper, Rep. Prog. Phys. **48**, 415 (1985).
[2] F. Bell, A.J. Rollason, J.R. Schneider, and W. Drube, Phys. Rev. B **41**, 4887 (1990).
[3] F.F. Kurp, M. Vos, Th. Tschentscher, A.S. Kheifets, J.R. Schneider, E. Weigold, and F. Bell, Phys. Rev. B **55**, 5440 (1997).
[4] Th. Tschentscher, J.R. Schneider, and F. Bell, Phys. Rev. B **48**, 16 965 (1993).
[5] M. Itou, S. Kishimoto, H. Kawata, M. Ozaki, H. Sakurai, and F. Itoh, J. Synchrotron Radiat. **5**, 676 (1998); J. Phys. Soc. Jpn. **68**, 515 (1999).
[6] R. Mayol and F. Salvat, At. Data Nucl. Data Tables **65**, 55 (1997).
[7] W.B. Pearson, *A Handbook of Lattice Spacings and Structures of Metals and Alloys* (Pergamon, New York, 1958).
[8] A. Bansil, Z. Naturforsch., A: Phys. Sci. **48a**, 165 (1993).
[9] A. Bansil, in *Electronic Band Structure and its Applications*, Lecture Note Series, Vol. 283, edited by M. Yussouff (Springer, Heidelberg, 1987), p. 273.
[10] J. Korringa, Physica (Utrecht) **13**, 391 (1947).
[11] W. Kohn and N. Rostoker, Phys. Rev. **94**, 1111 (1954).
[12] A. Bansil, L. Schwartz, and H. Ehrenreich, Phys. Rev. B **12**, 2893 (1975).
[13] A. Bansil, Phys. Rev. Lett. **41**, 1670 (1978).
[14] P.E. Mijnarends and A. Bansil, Phys. Rev. B **19**, 2912 (1979).
[15] A. Bansil, Phys. Rev. B **20**, 4035 (1979).
[16] A. Bansil, R.S. Rao, P.E. Mijnarends, and L. Schwartz, Phys. Rev. B **23**, 3608 (1981).
[17] P.E. Mijnarends, Phys. Status Solidi A **102**, 31 (1987).
[18] W.M. Temmerman, B.L. Gyorffy, and G.M. Stocks, J. Phys. F **8**, 2461 (1978).
[19] R. Benedek, R. Prasad, S. Manninen, B.K. Sharma, A. Bansil, and P.E. Mijnarends, Phys. Rev. B **32**, 7650 (1985).
[20] A. Bansil, S. Kaprzyk, A. Andrejczuk, L. Dobrzynski, J. Kwiatkowska, F. Maniawsky, and E. Zukowski, Phys. Rev. B **57**, 314 (1998).
[21] M.J. Puska and R.M. Nieminen, Rev. Mod. Phys. **66**, 841 (1994).
[22] B.W. Murray and J.D. McGervey, Phys. Rev. Lett. **24**, 9 (1970).
[23] L.J. Rouse and P.G. Varlashkin, Phys. Rev. B **4**, 2377 (1971).
[24] S. Tanigawa, S. Nanao, K. Kuribayashi, and M. Doyama, J. Phys. Soc. Jpn. **31**, 1689 (1971).
[25] S. Nanao, K. Kuribayashi, S. Tanigawa, and M. Doyama, Phys. Lett. **38A**, 489 (1972).
[26] M. Hasegawa, T. Suzuki, and M. Hirabayashi, J. Phys. Soc. Jpn. **37**, 85 (1974).
[27] E. Bruno, B. Ginatempo, E.S. Giuliano, A.V. Ruban, and Yu.Kh. Vekilov, Phys. Rep. **249**, 353 (1994).
[28] B.E.A. Gordon, W.E. Temmerman, and B.L. Gyorffy, J. Phys. F **11**, 821 (1981).
[29] P. Suortti and Th. Tschentscher, Rev. Sci. Instrum. **66**, 1798 (1995).
[30] A. Almazouzi, M.P. Macht, V. Naundorf, and G. Neumann, Phys. Rev. B **54**, 857 (1996).
[31] J.M. Poate, K.N. Tu, and J.W. Mayer, *Thin Films: Interdiffusion and Reactions* (Wiley, New York, 1978).
[32] H. Lefakes, J.F. Cain, and P.S. Ho, Thin Solid Films **101**, 207 (1983).
[33] R. Venos, W. Palmer, and H. Hoffmann, Thin Solid Films **162**, 155 (1988).
[34] B.C. Johnson, C.L. Bauer, and A.G. Jordan, J. Appl. Phys. **59**, 1147 (1986).
[35] A.D. LeClaire and G. Neumann, in *Diffusion in Solid Metals and Alloys*, edited by H. Mehrer, Landolt-Börnstein, New Series, Group III, Vol. 26, Chap. 3 (Springer, Heidelberg, 1990).
[36] H. Mehrer, in *Diffusion in Solid Metals and Alloys* (Ref. 35), Chap. 1.
[37] G. Brunel, G. Cizeron, and P. Lacombe, C. R. Seances Acad. Sci., Ser. B **269C**, 895 (1969).
[38] D.B. Butrymowicz, J.R. Manning, and M.E. Read, in *Diffusion Rate Data and Mass Transport Phenomena for Copper Systems, INCRA Series on the Metallurgy of Copper*, Vol. 5 (International Copper Research Association, New York, 1977).
[39] W. Assmann, J.A. Davies, G. Dollinger, J.S. Forster, H. Huber, Th. Reichelt, and R. Siegele, Nucl. Instrum. Methods Phys. Res. B **118**, 242 (1996).
[40] K. Wittmaack, in *Sputtering by Particle Bombardment III, Characteristics of Sputtered Particles, Technical Applications*, Topics in Applied Physics Vol. 64, edited by R. Behrisch and K. Wittmaack (Springer, Berlin, 1991), Chap. 4.
[41] M.L. Yu and W. Reuter, J. Appl. Phys. **52**, 1478 (1981).
[42] K. Wittmaack, Rev. Sci. Instrum. **47**, 157 (1976).
[43] K. Röll and W. Reill, Thin Solid Films **89**, 221 (1982).
[44] I. Suni, M.-A. Nicolet, and M. Mäenpää, Thin Solid Films **79**, 69 (1981).
[45] B. Mozer, D.T. Keating, and S.C. Moss, Phys. Rev. **175**, 868 (1968).
[46] J. Vrijen and S. Radelaar, Phys. Rev. B **17**, 409 (1978).
[47] B. Predel, in *Phase Equilibria, Crystallographic and Thermodynamic Data of Binary Alloys*, edited by O. Madelung, Landolt-Börnstein New Series, Group IV, Vol. 5d (Springer, Heidelberg, 1994), p. 203.
[48] L. Elford, F. Müller, and O. Kubaschewski, Ber. Bunsenges. Phys. Chem. **73**, 601 (1969).
[49] G. Kontrym-Sznadj, H. Stachowiak, W. Wierzchowski, K. Petersen, N. Thrane, and G. Trumpy, J. Appl. Phys. **8**, 151 (1975).
[50] A.P. Cracknell, in *Electron States and Fermi Surfaces of Elements*, edited by K.-H. Hellwege and J. L. Olsen, Landolt-Börnstein New Series, Group III, Vol. 13c (Springer, Heidelberg, 1984).

[51] S. Manninen, V. Honkimäki, K. Hämäläinen, J. Laukkanen, C. Blaas, J. Redinger, J. McCarthy, and P. Suortti, Phys. Rev. B **53**, 7714 (1996).
[52] A. Bansil and P.E. Mijnarends, Phys. Rev. B **30**, 628 (1984).
[53] C. Metz, Th. Tschentscher, P. Suortti, A.S. Kheifets, D.R. Lun, T. Sattler, J.R. Schneider, and F. Bell, J. Phys.: Condens. Matter **11**, 3933 (1999).
[54] W. Gudat and C. Kunz, Phys. Status Solidi B **52**, 433 (1972).
[55] N.F. Mott, Adv. Phys. **13**, 325 (1964).
[56] D.H. Seib and W.E. Spicer, Phys. Rev. B **2**, 1676 (1970); **2**, 1694 (1970).
[57] S. Hüfner, G.K. Wertheim, R.L. Cohen, and J.H. Wernick, Phys. Rev. Lett. **28**, 488 (1972).
[58] H.H. Hsieh, Y.K. Chang, W.F. Pong, J.Y. Pieh, P.K. Tseng, T.K. Sham, F. Coulthard, S.J. Naftel, J.F. Lee, S.C. Chung, and K.L. Tsang, Phys. Rev. B **57**, 15 204 (1998).
[59] N.N. Lathiotakis, B.L. Gyorffy, and J.B. Staunton, J. Phys.: Condens. Matter **10**, 10 357 (1998).
[60] S.N. Okuno and K. Inomata, Phys. Rev. Lett. **70**, 1711 (1993).
[61] I.M. Templeton and P.Z. Coleridge, J. Phys. F **5**, 1307 (1975).
[62] R. Prasad and A. Bansil, Phys. Rev. B **21**, 496 (1980).
[63] N.J. Shevchik and C.M. Penchina, Phys. Status Solidi B **70**, 619 (1975).